

Study of bound and resonance states of ^{11}Be in breakup reaction

D.S. Valiolda^{1,2,3}, D.M. Janseitov^{*,1,3,4}, V.S. Melezhik^{1,5}

¹Joint Institute for Nuclear Research, Dubna, Russia

²Al-Farabi Kazakh National University, Almaty, Kazakhstan

³Institute of Nuclear Physics, Almaty, Kazakhstan

⁴L.N. Gumilyov Eurasian National University, Astana, Kazakhstan

⁵Dubna State University, Dubna, Russian Federation

E-mail: d.janseit@inp.kz

DOI: 10.32523/ejpfm.2022060301

Received: 01.08.2022 - after revision

We investigate the Coulomb breakup of the ^{11}Be halo nuclei on a lead target within non-perturbative time-dependent approach in a wide range of beam energy (5–70 MeV/nucleon) including the low-lying resonances in different partial and spin states of ^{11}Be . We have found considerable contribution of the low-lying resonances ($5/2^+$, $3/2^-$ and $3/2^+$) to the breakup cross section of ^{11}Be . The obtained results are in good agreement with existing experimental data at 69 MeV/nucleon. The developed computational scheme opens new possibilities in investigation of Coulomb, as well as nuclear, breakup of other halo nuclei on heavy, as well as, light targets.

Keywords: halo nucleus; energy spectrum; Coulomb breakup; breakup cross section; low-lying resonances

Introduction

Since the discovery of radioactive secondary beams [1], exotic structures have been the subject of both theoretical and experimental intensive research [2]. In the study of halo nuclei, the Coulomb breakup cross section provides important information about the structure and characteristics of the halo system. Many theoretical approaches such as perturbation expansion [3, 4], adiabatic approximation [5], eikonal model [6], coupled-channels with a discretized continuum (CDCC) [7,

8], dynamical eikonal approximation (DEA) [9], numerical integration of a three-dimensional time-dependent Schrödinger equation (TDSE) [10-14] and others have been applied to breakup analysis of one-nucleon halo and two-nucleon halo nuclei.

In our recent work [15], the influence of resonance states ($5/2^+$, $3/2^-$ and $3/2^+$) to the Coulomb breakup of ^{11}Be nucleus on a heavy (^{208}Pb) target is investigated within the semiclassical and quantum-quasiclassical time-dependent approaches. The time-dependent Schrödinger equation is integrated with a non-perturbative algorithm on a three-dimensional spatial mesh. The method [10, 11, 15] makes use of values of the wave function at mesh points in angular space, in the spirit of the discrete-variable representation or Lagrange-mesh methods [16]. The radial functions are approximated with variable-step finite-difference techniques [11, 16]. Such a numerical technique has been successfully applied to the Coulomb breakup of loosely bound two-body systems like ^{11}Be [10, 11], ^{17}F [16], and ^{15}C [11] at intermediate beam energies.

Also, in [15] we extended theoretical model for breakup calculations by quantum-quasiclassical approach for lower beam energies (5–30 MeV/nucleon). It was shown that this numerical technique permits to include correctly the low-lying resonances in different partial and spin states of ^{11}Be in a wide range of beam energy (5–70 MeV/nucleon). Within the framework of that work [15], the main attention was paid to the calculations of the breakup cross section and it was not possible to consider in detail the computations of the energy levels of ^{11}Be nucleus.

In present work we describe in detail the calculation of the bound and resonant states of the ^{11}Be , which is an important element of the computational scheme. In addition in this paper we will discuss the parameterization of potential between the neutron and ^{10}Be core and how the resonant states were included in the analysis of the breakup reaction.

Theoretical description

The breakup reaction $^{11}\text{Be} + ^{208}\text{Pb} \rightarrow ^{10}\text{Be} + n + ^{208}\text{Pb}$ in the projectile rest frame by the time-dependent Schrödinger equation (TDSE):

$$i\hbar \frac{\partial}{\partial t} \Psi(\mathbf{r}, t) = H(\mathbf{r}, t) \Psi(\mathbf{r}, t) = [H_0(\mathbf{r}) + V_C(\mathbf{r}, t)] \Psi(\mathbf{r}, t) \quad (1)$$

where $\Psi(\mathbf{r}, t)$ is the wave packet of the neutron relative the ^{10}Be -core. Here

$$H_0(\mathbf{r}) = -\frac{\hbar^2}{2\mu} \Delta_{\mathbf{r}} + V(r) \quad (2)$$

$H_0(\mathbf{r})$ is the Hamiltonian describing relative halo nucleon-core motion with reduced mass $\mu = m_n m_c / M$, where m_n, m_c and $M = m_n + m_c$ are the neutron, ^{10}Be -core, and ^{11}Be masses, respectively.

The halo neutron is weakly bound to the ^{10}Be core nucleus treated as a structureless particle by the potential $V(r)$, which is the sum of an l -dependent

central potential $V_l(r)$ and a spin-orbit interaction $V_l^s(r)(\mathbf{ls})$. The interaction of the target nucleus with the projectile is described by the time-dependent Coulomb potential

$$V_C(\mathbf{r}, t) = \frac{Z_c Z_t e^2}{|m_n \mathbf{r} / M + \mathbf{R}(t)|} - \frac{Z_c Z_t e^2}{R(t)}, \quad (3)$$

where Z_c and Z_t are charge numbers of the core and target, respectively, and a straight-line trajectory $\mathbf{R}(t) = \mathbf{b} + \mathbf{v}_0 t$ is the relative coordinate between the projectile and the target, where \mathbf{b} is the impact parameter and \mathbf{v}_0 is the initial velocity of ^{11}Be relative Pb-target [10, 12-15].

The time evolution of $\Psi(\mathbf{r}, t)$ following from Eq. (1) is calculated according to the above scheme starting from the initial state $\Psi(\mathbf{r}, T_{in}) = \phi_{2s}$, where $\phi_{2s}(\mathbf{r})$ is the ground state of the ^{11}Be . Following the parameterization suggested in [17], the interaction $V(r)$ between the neutron and the ^{10}Be core is chosen for bound and resonance states as the sum of a spherical Woods-Saxon potential $V_l(r) = -V_l f(r)$, where $f(r) = 1/(1 + \exp((r - R_0)/a))$ and of a standard spin-orbit interaction

$$V_l^s(r) = V_{ls} \frac{1}{r} \frac{d}{dr} f(r)(\mathbf{ls}). \quad (4)$$

The standard value $V_{ls} = 21 \text{ MeV fm}^2$ is used for the depth of the ls potential for a p-shell nucleus [12]. The parameters of the Woods-Saxon potentials, as radius R_0 , diffuseness a and depth V_l are given in Table 1 and the selection of these parameters will be discussed further for bound and resonant states separately.

Table 1.
Parameters of the potentials.

$V_{l,even}$ (MeV)	$V_{l,odd}$ (MeV)	V_{ls} (MeV fm ²)	a (fm)	R_0 (fm)	States
62.52	39.74	21.0	0.60	2.585	$1/2^\pm, 5/2^+, 3/2^+$
	6.80	21.0	0.35	2.500	$3/2^-$

The eigenfunctions of Hamiltonian H_0 with energy E are denoted as $\phi_{ljm}(E, \mathbf{r})$,

$$H_0(\mathbf{r})\phi_{ljm}(\mathbf{r})(E, \mathbf{r}) = E\phi_{ljm}(E, \mathbf{r}) \quad (5)$$

here j is a projectile total momentum $j = l + s$, resulting from the coupling of the orbital momentum l and spin s of the neutron, m is a magnetic quantum number.

For discretizing with respect to the radial variable r , a sixth-order (seven point) finite-difference approximation on a quasiuniform grid has been used on the interval $r \in [0, r_m]$ with $r_m = 1200 \text{ fm}$. The grid has been realized by mapping $r \rightarrow x$ the initial interval onto $x \in [0, 1]$ by the formula $r = r_m(e^{8x} - 1)/(e^8 - 1)$ [11, 16]. The stationary Schrödinger equation (5) and the TDSE (1) are solved on the same quasiuniform radial grid.

All details of the numerical solution of the Schrödinger equation, the convergence and accuracies of the computational scheme are described at [10, 11, 15].

The parameterization of the interaction between the neutron and core

In this section we describe in detail the selection of parameters of the spherical potential $V_l(r) = -V_l/(1 + \exp((r - R_0)/a))$, describing the energy spectrum of ^{11}Be nucleus, which was previously used in [15], but it was not possible to discuss it minutely at [15].

The depths of the Woods-Saxon potentials have been determined as $V_l = 62.52$ MeV (l -even) and $V_l = 39.74$ MeV (l -odd) [9] in order to reproduce the $1/2^+$ ground state of ^{11}Be at -0.503 MeV, the $1/2^-$ excited state at -0.183 MeV and two resonance states $5/2^+$ and $3/2^+$ with the position of peaks at $E(5/2^+) = 1.232$ MeV and $E(3/2^+) = 3.367$ MeV [18, 19]. As it is shown in Table 1 for all these states, except the resonance $3/2^-$, the radius is $R_0 = 2.585$ fm and the diffuseness is $a = 0.6$ fm.

Thus, in solving of the radial Schrödinger equation (5) for a neutron-core system four set of potentials were used. In the discrete spectrum the parameter $V_l = 62.52$ MeV of the Woods-Saxon potential reproduces ground state at $E = -0.503$ MeV ($l=0, 1/2^+$) and the depth $V_l = 39.74$ MeV describes the first excited state ($l=1, 1/2^-$). In the continuous spectrum ($E > 0$) for $l=2$ with the set of parameter $V_l = 62.52$ MeV from [9], we got the positions of two resonances $3/2^+$ ($l-1/2$) and $5/2^+$ ($l+1/2$) as $E(5/2^+) = 1.232$ MeV and $E(3/2^+) = 3.367$ MeV [18, 19]. To fix the position of the $3/2^-$ resonance ($l=1$) close to the theoretical [18] and experimental [19] value $E(3/2^-) = 2.789$ MeV, we tuned the set of parameters V_l , a and R_0 ourselves (see Table 1) at our recent investigation [15], since the parameters of [9] do not reproduce the position of resonance $3/2^-$. For $l \geq 3$, the spherical potential $V(r)$ was set to zero.

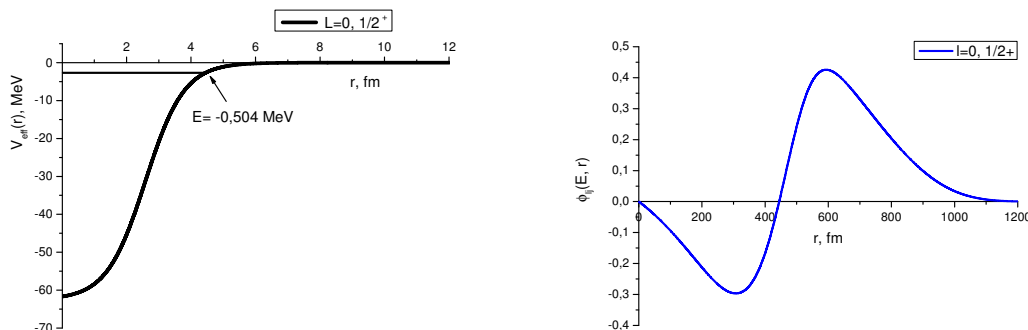


Figure 1. The effective potential and radial part $\phi_{lj}(E, r)$ of the ground state ($1/2^+$) of ^{11}Be ($l=0$) wave function.

In Figure 1 we present the radial part $\phi_{lj}(E, r)$ of the ground state ($1/2^+$) of ^{11}Be wave function $\phi_{lj}(E, \mathbf{r}) = \phi_{lj}(E, r)Y_{lm}(\hat{r})$, which is the solution of the eigenvalue problem (5) with $l=0$ at discrete spectrum normalized to unity

($\int(\phi_{lj}(E,r))^2 dr = 1$). Here the internal Hamiltonian $H_0(\mathbf{r})$ (2) includes potentials, the summation of which translates the so-called effective potential of the relative neutron-core motion, with the parameterization for $l=0$ discussed above. The effective potential (see Figure 1)

$$V_{eff} = V_l(r) + V_l^s(r)ls + \frac{\hbar^2 l(l+1)}{2\mu r^2} \quad (6)$$

consists of a Woods-Saxon potential $V_l(r)$, a spin orbital term of interaction $V_l^s(r)ls$ and centrifugal barrier .

For the case with the orbital momentum $l=1$, two sets of parameters were used for discrete ($l-1/2$) and continuous ($l+1/2$) spectrum. As it is shown in Figure 2 (a), the position of the $3/2^-$ resonance (red line) overtop the shape of the potential, calculated with the set of parameters from [9], which shows the feasibility of selecting the potential by ourselves at [15] for this level.

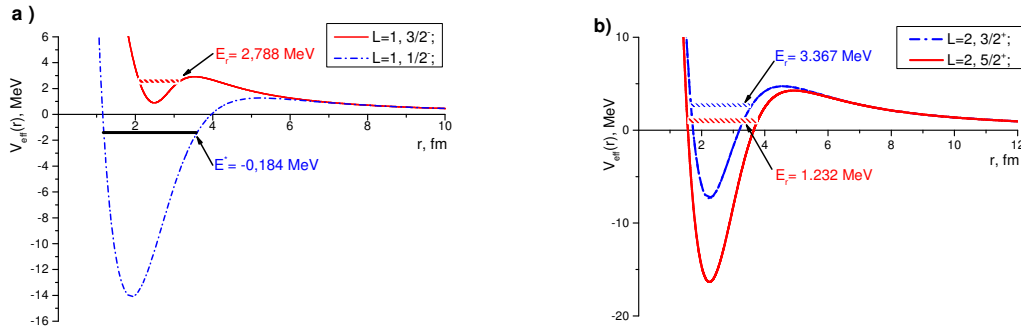


Figure 2. a) The effective potential, describing first excited $1/2^-$ state ($l-1/2$) at $E=-0.184$ MeV and resonance $3/2^-$ ($l+1/2$) with the position $E=2.788$ MeV ($l=1$). b) The effective potential, calculated for $l=2$ to reproduce the resonances $3/2^+$ ($l-1/2$) with the position of the energy $E=3.367$ MeV (blue dashed dots) and $5/2^+$ ($l+1/2$) state with the peak at $E=1.232$ MeV (red line).

Performing integration of the eigenvalue scattering problem (Eq. 5 when $E > 0$) for $l=2$ with the parameters $V_l = 62.52$ MeV, $R_0 = 2.585$ fm and $a = 0.6$ fm, we reproduce the position of peaks at $E(5/2^+) = 1.232$ MeV and $E(3/2^+) = 3.367$ MeV [18, 19], which is shown in Figure 2 b).

The radial p-wave function $\phi_{lj}(E,r)$ of excited ($1/2^-$) bound state (blue line in Figure 3a)) and scattering p3/2 wave function (red line in Figure 3b)) $\phi_{lj}(E,r)$ in the continuum are the solutions of the eigenvalue problem (5) on the same radial grid. The radial wave functions of a d3/2 and d5/2 scattering states are plotted at c) and d) part of Figure 3.

The scattering states are computed at energies corresponding to the positions of the three resonances $3/2^-$, $3/2^+$ and $5/2^+$. The radial part of the eigenfunction of the Hamiltonian $H_0(\mathbf{r})$ (5) $\phi_{lj}(kr)$ in the continuum spectrum ($E > 0$) is normalized $\phi_{lj}(kr) \rightarrow 0$, if $kr \rightarrow 0$ in accordance with the boundary condition $\phi_{lj}(kr) \rightarrow \frac{\sin(kr - \frac{\pi l}{2})}{k}$, if $kr \rightarrow \infty$.

Thus, we present here our numerical results of calculation of the bound and continuum resonant states of $H_0(\mathbf{r})$, which is a necessary initial value for integration of time-dependent Schrödinger equation (1) and breakup analysis of halo nuclei.

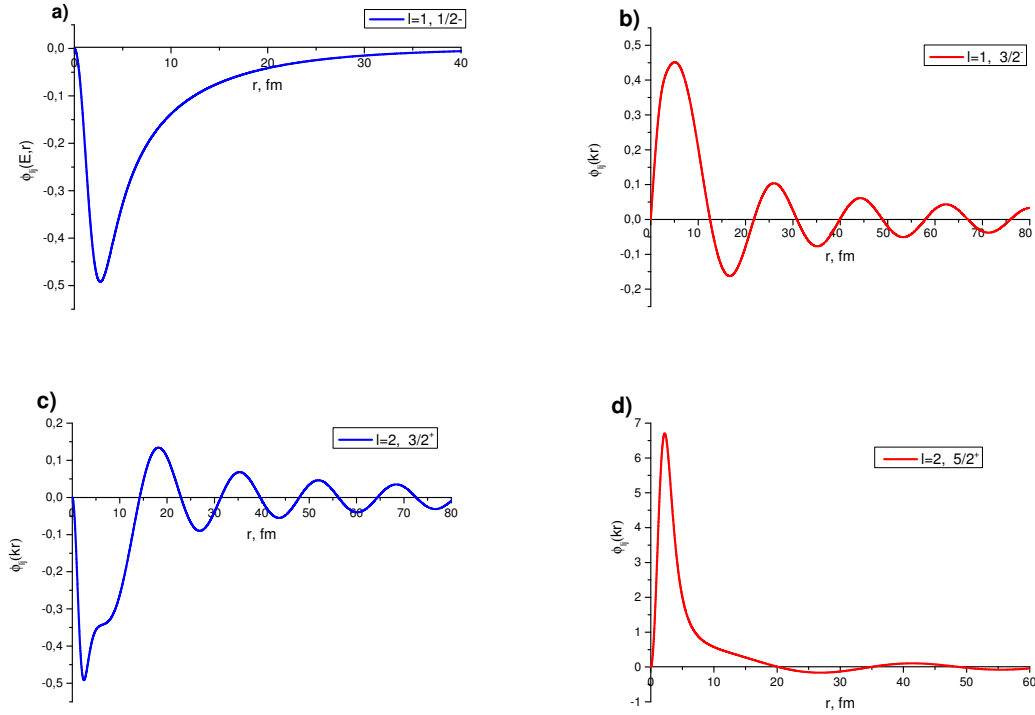


Figure 3. The radial part of p1/2 wave function $\phi_{lj}(E, r)$ of excited ($1/2^-$) bound state (a) of discrete spectrum and scattering p3/2 wave function $\phi_{lj}(kr)$ in the continuum (b) ($l=1$), scattering d3/2 and d5/2 wave functions $\phi_{lj}(kr)$ of $3/2^+$ (c) and $3/2^+$ (d) resonances ($l=2$).

Cross section of the breakup reaction

The total cross section of the breakup reaction $^{11}\text{Be} + ^{208}\text{Pb} \rightarrow ^{10}\text{Be} + n + ^{208}\text{Pb}$ is calculated as a function of the relative energy between the emitted neutron and the core nucleus including neutron interaction with the core in the final state of the process:

$$\frac{d\sigma_{bu}(E)}{dE} = \frac{4\mu k}{\hbar^2} \int_{b_{min}}^{b_{max}} \sum_{j=l+s} \sum_{lm} \left| \int \phi_{lj}(kr) Y_{lm}(\hat{r}) \Psi(\mathbf{r}, T_{out}) d\mathbf{r} \right|^2 b db \quad (7)$$

Here $\phi_{ljm}(kr)$ is the radial part of the eigenfunction of the Hamiltonian $H_0(\mathbf{r})$ (5) in the continuum spectrum ($E = k^2 \hbar^2 / (2\mu) > 0$), normalized to spherical Bessel function $j_l(kr)$ as $kr \rightarrow \infty$. The summation over (l, m) in (6) includes all 16 partial waves up to $l_{max} = 3$ inclusive [15].

Time evolution starts at initial time T_{in} and stops at final time T_{out} by iteration over N_T time steps Δt as explained in [11]. The initial (final) time T_{in} (T_{out}) has to be sufficiently big $|T_{in}|, T_{out} \rightarrow +\infty$, from the demand for the time-dependent potential $V_C(\mathbf{r}, t)$ to be negligible at the beginning (end) of the evolution process. We select the same time interval: $T_{in} = -20 \hbar / \text{MeV}$ and $T_{out} = 20 \hbar / \text{MeV}$, and fixed time step $\Delta t = 0.01 \hbar / \text{MeV}$ as in Ref. [10, 11].

Investigation of the halo nuclei through the Coulomb breakup of the system is important. As it is known, experiments for the breakup reaction $^{11}\text{Be} + ^{208}\text{Pb} \rightarrow ^{10}\text{Be} + n + ^{208}\text{Pb}$ [20, 21] were performed at intermediate beam energies (69 and 72 A MeV) and many theoretical calculations and processing [9-12, 17] were

made taking into account only bound states. In our recent work [15] we have investigated the influence of low-lying resonances of ^{11}Be into breakup reactions, and here we would like to show how the inclusion of resonances and the nuclear interaction effects contribute to the cross section of the Coulomb breakup.

The interaction $V_C(\mathbf{r}, t)$ of the target with the projectile (discussed at previous section) assumed to be purely Coulombic (3) and the nuclear interaction effects were simulated by a cutoff $b_{min} = 12$ fm at the Eq. (6). Including of nuclear interaction between the projectile and the target afford to make a calculations with smaller impact parameters starting with $b_{min} = 5$ fm [15]. In this section we study the contribution of the nuclear part of the projectile-target interaction in the breakup cross sections at low beam energies.

Following [11], the optical potential for the nuclear part $\Delta V_N(\mathbf{r}, t) = V_{cT}(r_{cT}) + V_{nT}(r_{nT})$ between the target and projectile-nucleus interaction is:

$$V(\mathbf{r}, t) = V_C(\mathbf{r}, t) + \Delta V_N(\mathbf{r}, t). \quad (8)$$

here r_{cT} and r_{nT} are the core-target $\mathbf{r}_{cT}(t) = \mathbf{R}(t) + m_n\mathbf{r}/M$ and neutron-target $\mathbf{r}_{nT}(t) = \mathbf{R}(t) - m_c\mathbf{r}/M$ relative variables and optical potentials V_{cT} and V_{nT} have the form:

$$V_{xT}(r_{xT}) = -V_x f(r_{xT}, R_R, a_R) - iW_x f(r_{xT}, R_I, a_I) \quad (9)$$

with Woods-Saxon form factors $f(r_{xT}, R_R, a_R) = 1/(1 + \exp(r_{xT} - R)/a)$, where x stands for either core or neutron. We use here the parameters of the optical potential from the earlier work [11].

Figure 4 illustrates the calculations of breakup cross section with pure Coulomb (3) and additional nuclear part of interaction (7) for lower beam energy of 10 MeV/nucleon taking into account bound and three resonant states. Also the results obtained by Coulomb potential (3) with considering only two bound states are given for comparison. It is shown that the cutoff Coulomb approximation (3) underestimates the breakup cross section including the nuclear interaction between the projectile and the target (7) and the inclusion of three resonance states into the breakup reaction considerably corrects the breakup cross sections, especially near the resonant energy 1.23 MeV of the $5/2^+$ resonance.

It can be seen that with a decreasing of beam energy, the influence of the nuclear effect in the projectile-target interaction becomes more significant for the breakup cross section. The contribution from the resonance states remains noticeable when the nuclear interaction between the target and the projectile is included, and the peak due to the $5/2^+$ resonance is clearly visible at low beam energies.

Conclusion

This work is a kind of addition to our recently published new results in [15], where we for the first time included low-lying resonant states of the ^{11}Be nucleus in the calculation of the breakup cross section and extended the theoretical model

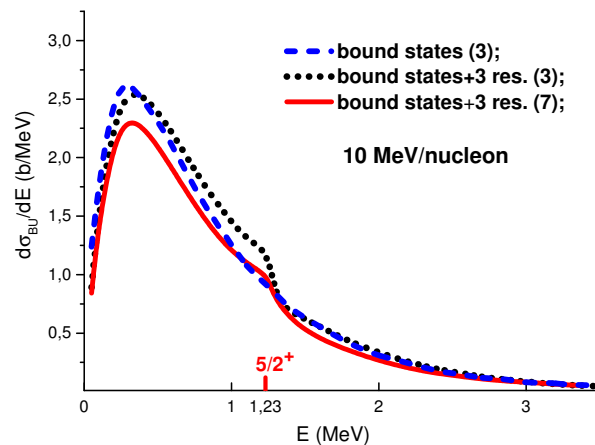


Figure 4. Breakup cross sections calculated with only bound states (dotted curve) in the interaction between the neutron and the ^{10}Be -core and taking into account three resonant states (dashed curves) for pure Coulomb potential (3) and with (7) adding of nuclear interaction (full lines) between the projectile and target for the case of including both bound and resonant states ($5/2^+$, $3/2^-$, $3/2^+$ at 10 MeV/nucleon).

to low beam energies. Unfortunately, in that work [15] it was not possible to describe in detail how these resonances were included in the numerical technique.

Here we describe in depth the results of calculating the spectrum and resonant states of the ^{11}Be , which is an important element of the computational scheme. In this paper we paid attention to discuss the parameterization of potential between the neutron and ^{10}Be core and illustrate these internal effective potential for different partial and spin states of the ^{11}Be nucleus.

As an example for a low beam energy at 10 MeV/nucleon, we showed a noticeable contribution from the low-lying resonances ($5/2^+$, $3/2^-$ and $3/2^+$) and the influence of nuclear effects in the interaction of the projectile with the target. In particular, the contribution of the $5/2^+$ resonance state of ^{11}Be to the breakup cross sections is clearly visible at low energies.

The method can potentially be useful for interpretation and planning of low-energy Coulomb, as well as nuclear breakup experiments on different targets in studying the halo nuclei.

Acknowledgments

This research is funded by the Science Committee of the Ministry of Education and Science of the Republic of Kazakhstan (Grant No. AP13067742).

References

- [1] I. Tanihata, J. Phys. G **22** (1996) 157. [[CrossRef](#)]
- [2] K.A. Kuterbekov, A.M. Kabyshev, A.K. Azhibekov, Chinese Journal of Physics **55** (2017) 2523-2539. [[CrossRef](#)]
- [3] S. Typel, G. Baur, Phys. Rev. C **50** (1994) 2104. [[CrossRef](#)]
- [4] H. Esbensen, G.F. Bertsch, Nucl. Phys. A **600** (1996) 37. [[CrossRef](#)]

- [5] J.A. Tostevin, S. Rugmai, R.C. Johnson, Phys. Rev. C **57** (1998) 3225. [[CrossRef](#)]
- [6] Y. Suzuki et al., Structure and Reactions of Light Exotic Nuclei (Taylor & Francis, London, 2003) 608 p. [[CrossRef](#)]
- [7] M. Kamimura et al., Prog. Theor. Phys. Suppl. **89** (1986) 1–10. [[CrossRef](#)]
- [8] J.A. Tostevin, F.M. Nunes, I.J. Thompson, Phys. Rev. C **63** (2001) 024617. [[CrossRef](#)]
- [9] D. Baye, P. Capel, G. Goldstein, Phys. Rev. Lett. **95** (2005) 082502. [[CrossRef](#)]
- [10] V.S. Melezhik, D. Baye, Phys. Rev. C **59** (1999) 3232. [[CrossRef](#)]
- [11] P. Capel, D. Baye, V.S. Melezhik, Phys. Rev. C **68** (2003) 014612. [[CrossRef](#)]
- [12] T. Kido, K. Yabana, Y. Suzuki, Phys. Rev. C **50** (1994) R1276. [[CrossRef](#)]
- [13] H. Esbensen, G.F. Bertsch, C.A. Bertulani, Nucl. Phys. A **581** (1995) 107. [[CrossRef](#)]
- [14] A.K. Azhibekov, V.V. Samarin, K.A. Kuterbekov, Chinese Journal of Physics **65** (2020) 292-299. [[CrossRef](#)]
- [15] D. Valiolda, D. Janseitov, V.S. Melezhik, European Physical Journal A **58** (2022) 34. [[CrossRef](#)]
- [16] V.S. Melezhik, Phys. Lett. A **230** (1997) 203. [[CrossRef](#)]
- [17] P. Capel, G. Goldstein, D. Baye, Phys. Rev. C **70** (2004) 064605. [[CrossRef](#)]
- [18] S.N. Ershov, J.S. Vaagen, M.V. Zhukov, Phys. of Atomic Nucl. **77** (2014) 989. [[CrossRef](#)]
- [19] National Nuclear Data Center. [[Weblink](#)]
- [20] T. Nakamura et al., Phys. Lett. B **394** (1997) 11. [[CrossRef](#)]
- [21] N. Fukuda et al., Phys. Rev. C **70** (2004) 054606. [[CrossRef](#)]